ACS OMEGA

Open Access

http://pubs.acs.org/journal/acsodf

Article

Novel Thermosensitive Hydrogel Encapsulated Carvedilol for the Treatment of Rosacea

Huiya Chen, Zhigang Zhang, Jue Qi, Can Cao, Min Lin, Lechun Lyu,* and Dan Xu*

Cite This: *ACS Omega* 2025, 10, 7964−7972

Read Online

ACCESS | Metrics & More | Article Recommendations

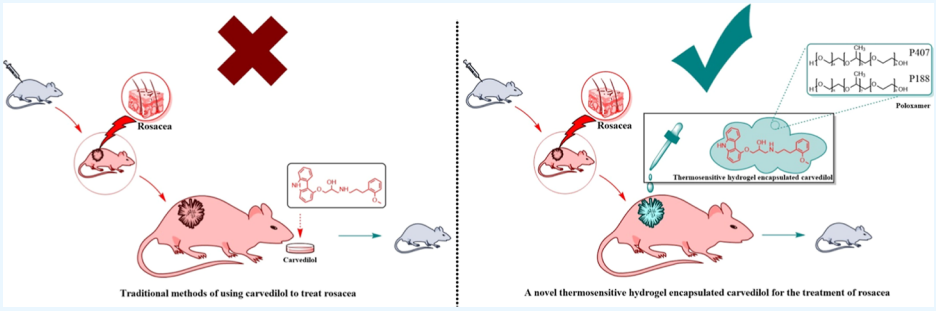

ABSTRACT: Background: Carvedilol can be used in the treatment of rosacea. However, their oral administration often results in a series of adverse effects. Purpose: A novel thermosensitive hydrogel was developed to improve the administration of carvedilol in the treatment of rosacea and to evaluate its safety and efficacy. Methods: The thermosensitive hydrogel was formulated using varying ratios of poloxamer 407 (P407) and poloxamer 188 (P188), with carvedilol being encapsulated during the process. The gel temperature and time of the hydrogel were observed, its phase transition was assessed through the inverted tube test, its microstructure was examined using scanning electron microscopy (SEM), and its characteristic functional groups were identified with Fourier transform infrared spectrometry (FTIR). The hydrogel's therapeutic efficacy on a rosacea-like phenotype in mice was evaluated through in vitro experiments. Results: It is observed that the microstructure of the hydrogel possesses a porous structure, with pores uniformly arranged in a square lattice measuring 8−12 μm in diameter. Thermosensitive hydrogel encapsulated carvedilol (Car-P407$_{24}$/P188$_1$) had favorable drug release rate and swelling properties. Live/dead cell assays indicated minimal toxicity of the hydrogel to HaCaT cells, and the carvedilol encapsulated with hydrogel possessed a better therapeutic effect on the rosacea-like phenotype in mice. Conclusion: Car-P407$_{24}$/P188$_1$ was not significantly cytotoxic and possessed good cellular biocompatibility. Furthermore, it exhibits a good therapeutic effect on rosacea-associated facial flushing and erythema. It possesses some anti-inflammatory properties and exhibits great potential for future use in rosacea treatment.

1. INTRODUCTION

Rosacea is a chronic inflammatory skin disease, mostly occurring in the middle of the face, mainly manifested as paroxysmal flushing of the skin and persistent erythema. In severe cases, there will be papules, pustules, and capillary dilatation. Additionally, some patients may have hyperplasia and hypertrophy and ocular changes.[1−4] An investigation suggests that the global prevalence of rosacea is around 5.46%. A survey from 2019 to 2020 showed that the prevalence rate of rosacea in China was about 3.4%.[5−7] Fixed central facial erythema is considered to be the diagnostic phenotype of rosacea,[8] while flushing and erythema are the most common manifestations of all types of rosacea. The high recurrence of flushing and erythema, especially on the face, has a significant impact on the patient's psychology and quality of life;[9−11] improving patients' flushing and erythema still remains a great challenge in clinic.[12,13]

Carvedilol is a α1-receptor antagonist and a nonselective β-receptor antagonist, which is recommended for the treatment of flushing and persistent erythema in rosacea.[14−17] The mechanism is thought to involve contraction of smooth muscle in small cutaneous arteries by blocking β2-adrenergic receptors.[18] In addition, carvedilol slows cardiac function by blocking cardiac β2-adrenergic receptors, further improving refractory facial flushing and persistent erythema.[19] Moreover, carvedilol possesses additional antioxidant and anti-inflammatory effects compared with other nonselective β-blockers.[20,21]

Received: September 28, 2024
Revised: January 30, 2025
Accepted: February 4, 2025
Published: February 19, 2025

It could also relieve flushing and erythema caused by rosacea through down-regulate TLR2/KLK5/catheterin pathway.[20]

It is worth noting that the target of action of carvedilol is widely distributed, which makes it easy for oral administration to cause serious adverse reactions,[14] which has hampered its further use in the clinic. Adjustments to the mode of administration and route of drug delivery of carvedilol are urgent issues to be addressed. To enhance the bioavailability of carvedilol, several methods for improving the delivery of carvedilol have been developed in the past few years, primarily for hypertension-related research.[22,23] Currently, topical medications targeted at treating erythema and flushing caused by rosacea include brimonidine (α2-adrenoceptor agonist) and oxymetazoline (α1-adrenoceptor agonist).[24] In contrast, research on carvedilol as a topical dosage form for the treatment of rosacea has not yet been reported yet.

Hydrogels, using water as a medium, possess the characteristics of high water retention, water absorption, and slow release. Thermosensitive hydrogels are one of the many classifications of hydrogels. Currently, thermosensitive hydrogels are widely researched and applied in many fields such as drug slow control, tissue engineering, and cell engineering.[25] Thermosensitive hydrogels can be divided into natural thermosensitive hydrogels and synthetic thermosensitive hydrogels. Poloxamer is a typical synthetic thermosensitive hydrogel;[26] it is a polyoxyethylene (PEO)−polyoxypropylene (PPO) block copolymer. PEO possesses good hydrophilicity, PPO possesses good hydrophobicity, and the copolymer formed by chimerization of them possesses a unique hydrophilic outer shell and internal hydrophobicity, which makes it possible to encapsulate both hydrophilic and hydrophobic drugs. Moreover, the three-dimensional structure formed by the chimera can form a good drug reservoir.[27−30] In addition, poloxamer possesses a good property of phase transition, with the lowest cosolubilization temperature as the critical threshold, and the temperature is adjusted to achieve sol−gel transition. The phase transition temperature and stability of the gel can be improved by adjusting the mixing ratio of poloxamer 407 (P407) and poloxamer 188 (P188).[31] Therefore, it can be used as a good support for topical dosage forms of carvedilol.

In this work, P407 and P188 were blended to make a thermosensitive hydrogel, encapsulating carvedilol for the treatment of rosacea-induced flushing and erythema. Materials were characterized using scanning electron microscopy (SEM) and Fourier transform infrared (FTIR) spectroscopy. It has been verified that the topical drug possesses good biocompatibility and shows significant effects on flushing and erythema caused by rosacea while also possessing a certain anti-inflammatory effect. This work sheds new light on the development of topical dosage forms for the treatment of rosacea.

2. MATERIAL AND METHODS

2.1. Chemicals and Reagents. Carvedilol (purity; 98%) was purchased from Shanghai Xianding Biotechnology. P407 and P188 were purchased from Solarbio Co., Ltd. (Shanghai, China). Other AR-grade chemicals were obtained from Aladdin Biochemical Technology Co., Ltd. (Shanghai, China) and Sangon Biotech Co., Ltd. (Guizhou, China).

2.2. Preparation of the Hydrogel. P407 and P188 were mixed in a 50 mL centrifuge tube, and 20 mL of deionized water was added to it to form a mixture of different concentrations, which was put into a 4 °C refrigerator. This was observed every 12 h and mixed fully upside down until a colorless and transparent poloxamer sol was obtained, which was kept in the refrigerator at 4 °C for spare use. Carvedilol powder was weighed and dissolved completely in DMSO to obtain a carvedilol solution. Different volumes of prepared carvedilol solution were pipetted into the mixture of P407 and P188 to obtain different contents of Car-P407$_x$/P188$_y$ (x = 23, 24, 25 wt %, y = 0.5, 1.0, 1.5 wt %), which were placed in a refrigerator at 4 °C to fully dissolve and mix until the sol was clarified and transparent.

2.3. Characterization and Detection of Thermosensitive Hydrogels. Hydrogel lyophilizates were prepared by the freeze-drying method, and then, the blank hydrogel and the hydrogel containing the drug were scanned with a scanning electron microscope (Hitachi-TM1000, Hitachi, Japan) in the range of 50−100 μm. Blank and drug-containing hydrogels were measured using a FTIR spectrometer (TENSOR-27, Bruker, Germany) with a resolution of 4 cm^{-1} and a frequency range of 500−4000 cm^{-1}.

2.4. Stirring and Inversion Method. The gel time was determined by using the stirring method. The prepared gel aqueous solution was placed in a water bath preset to a specific temperature, and the temperature of the magnetic stirrer was set so that the time when the magnetic stirrer stopped rotating was taken as the gel time.

The gel temperature was determined by using the inversion method. The prepared gel aqueous solution was placed in an incubator and gradually heated, with the heating rate controlled at 1 °C per 2 min. Every 10 min, the solution was inverted and tilted at a 60° angle to the ground. The solution was considered to have gelled if it did not flow within 30 s, and the gel temperature was recorded.

2.5. Swelling Test. An appropriate amount of phosphate buffered saline (PBS) at 37 °C was added to the freeze-dried hydrogel lyophilizate, placed in a 37 °C warming chamber for adequate dissolution, and weighed at various time points. Percentage swelling rate (SR) was calculated according to eq 1, where W_d is the initial dry weight of the hydrogel and W_w is the weight of the hydrogel after swelling in PBS. The calculation formula is as follows

$$\text{dissolution rate } (\%) = [(W_W - W_d)/W_d] \times 100\% \quad (1)$$

2.6. Carvedilol Release Trial. The gel with different proportions of 2 mL was added with 5 mL of pH 7.4 PBS and 0.2 wt % Tween 20. It was kept away from light in a constant temperature shaker (100 rpm) and placed at 37 °C for 96 h. The UV absorbance at 285 nm of PBS in the test tubes was measured at different time points. Cumulative drug release rate was calculated for drug release studies.

2.7. In Vitro Cytotoxicity. Human keratinocytes (HaCaT) were cultured in Dulbecco's modified Eagle's medium (Sigma-Aldrich) containing 10% heat-inactivated fetal bovine serum (Gibco American). Cells were incubated in a 95% atmosphere and 5% CO_2 at 37 °C. After the cells had grown to a suitable density, different drug-containing hydrogels were added and cocultured for a certain period of time. Cells were labeled with an FDA/propidium iodide (PI) staining cytotoxicity kit (Beyotime, Shanghai, China), and cell viability was detected by fluorescence microscopy (IX73, OLYMPUS, Japan).

2.8. Experimental Animals and Treatments. Female BALB/c mice (6−7 weeks, weights of 18−25 g) were provided by the Experimental Animal Center of Kunming Medical

https://doi.org/10.1021/acsomega.4c08884
ACS Omega 2025, 10, 7964−7972

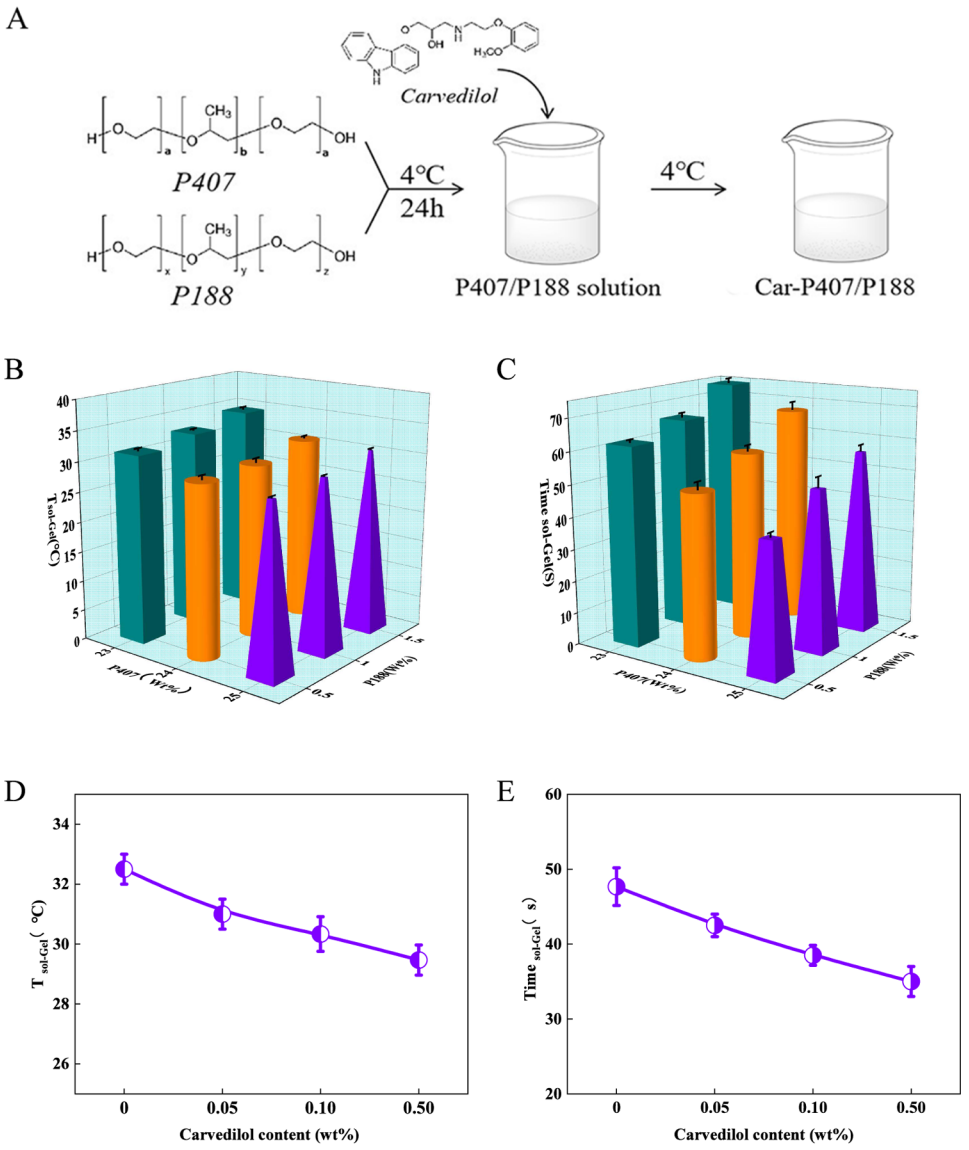

Figure 1. Preparation and optimization of conditions for thermosensitive hydrogels containing carvedilol. (A) Preparation of thermosensitive hydrogels encapsulating carvedilol, effect of changing the P407 and P188 content on the temperature (B) and time (C) of the sol−gel phase transition, and effect of different drug-containing gels on the temperature (D) and time (E) of the phase transition.

University. Laboratory animals were approved by Kunming Medical University's Animal Ethics Committee, under the guidelines of its ethics committee. Mice were anesthetized by intraperitoneal injection of sodium pentobarbital (50 mg/kg), and the hair on the upper back was shaved. An antimicrobial peptide (LL37) was used to induce a rosacea-like mouse. Mice were injected twice daily with 40 μL of LL-37 (320 μM) intradermally for 2 days at the marked back positions. The mice were randomly divided into 4 groups: control, PBS, LL37, and LL37 + drug-containing gel, with 10 mice in each group. No other treatment was performed in the control group. PBS was injected in the back in the PBS group, LL37 was injected in the back in the LL37 group and LL37 + drug-containing gel group, and the LL37 + drug-containing gel group was injected with LL37, with the drug-containing gel applied to the back. Photographs were taken 12 h after the last injection, and mice were executed under anesthesia 4 days later to dissect the diseased skin tissue for histological analysis.

2.9. Skin Condition Analysis. The backs of the mice were photographed with a digital camera 12 h after completion of the injection and 4 days after the treatment. Erythema was observed with a dermatoscopic image processing workstation, and the skin condition was observed with a body-reflective confocal microscope.

2.10. HE Staining. Four days after injection, the skin tissue was collected, fixed in 4% paraformaldehyde, dehydrated, and embedded in paraffin. Successive 5 μm tissue sections were cut with a microtome (LeicaCM1950, Germany), followed by HE staining to observe the morphological features of the tissues. Images of each section were acquired by using a light microscope (OlympusCX40, Japan).

2.11. Statistical Analysis. All statistical analyses were carried out by using the statistical software SPSS 26.0. All quantitative data presented in this study were expressed as mean (±) standard deviation. $\rho < 0.05$ was considered statistically significant. Graphs were plotted using OriginPro 2021.

https://doi.org/10.1021/acsomega.4c08884
ACS Omega 2025, 10, 7964−7972

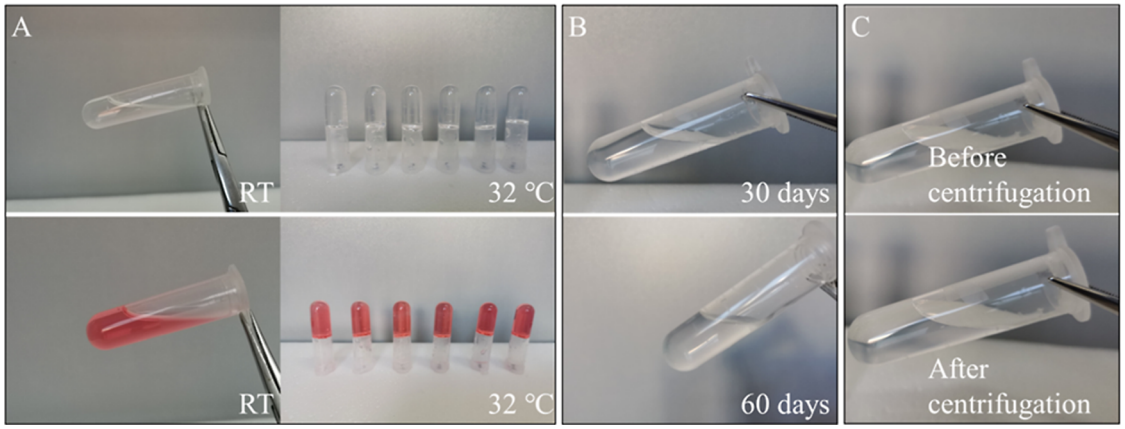

Figure 2. Stability testing of Car-P407$_{24}$/P188$_1$. (A) Tube inversion experiments and (B) gel states of drug-containing gels left at room temperature for 30 days and 60 days and (C) after ultrahigh speed centrifugation.

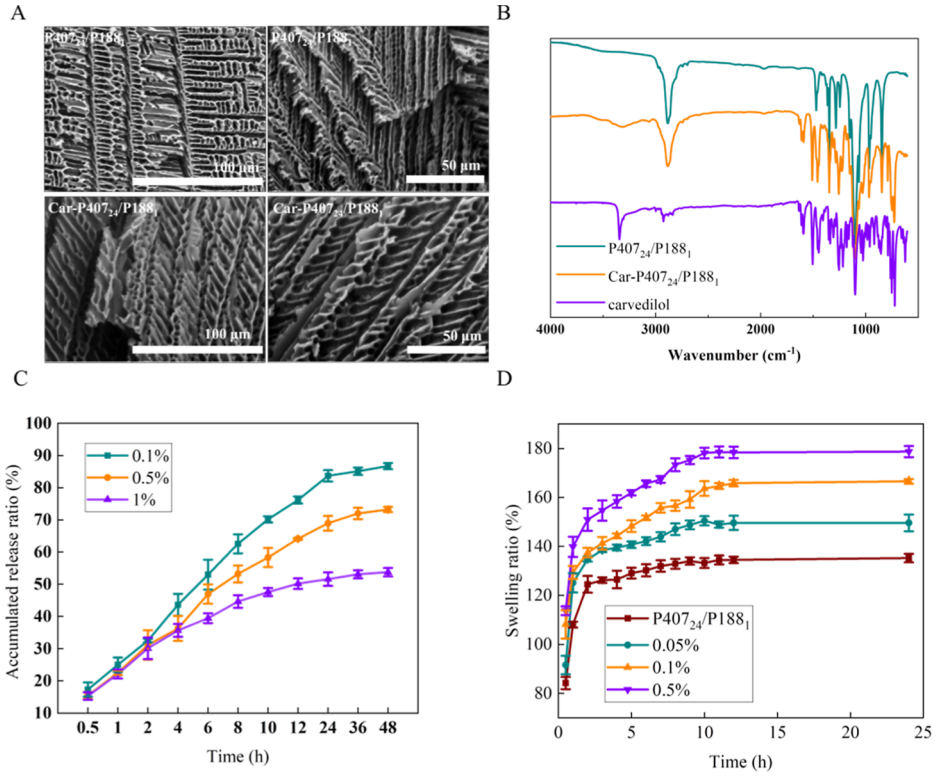

Figure 3. Characterization of P407$_{24}$/P188$_1$ and Car-P407$_{24}$/P188$_1$. (A) Scanning electron micrographs of P407$_{24}$/P188$_1$ and Car-P407$_{24}$/P188$_1$ and (B) FTIR, (C) cumulative drug release rate from drug-containing gel, and (D) SR of the drug-containing gel.

3. RESULTS

3.1. Preparation of the Car-P407/P188 Hydrogel. The synthetic process for thermosensitive hydrogel encapsulating carvedilol is shown in Figure 1A. Figure 1B,C shows the effect of changing the P407 and P188 content on the temperature and time of the sol−gel phase transition, respectively. It could be found that the change in the mass fraction of P407 and P188 affects the phase transition temperature and phase transition time. Fixing the mass fraction of P407 and increasing the mass fraction of P188, the phase transition temperature increased and the phase transition time prolonged. Fixing the mass fraction of P188 and increasing the mass fraction of P407, the phase transition temperature increased and the phase transition time shortened. Considering that the exposed skin temperature was roughly 32−36 °C, P407$_{24}$ (24 wt %) and P188$_1$ (1.0 wt %) were finally selected, which possessed a gel temperature of 30−35 °C and a molding time of 30−90 s (Figure 1B,C).

P407$_{24}$/P188$_1$ was used as drug encapsulants to prepare thermosensitive hydrogels encapsulating 0.05, 0.1, and 0.5 wt % carvedilol. Figure 1D,E shows the effect of different drug-containing gels on the temperature and time of the phase transition, respectively. The gel formation time of the thermosensitive composite hydrogel at the same temperature was shortened by the addition of different amounts of carvedilol to the poloxamer hydrogels, and the carvedilol solution altered the gel formation time and gel formation temperature of the system to a small extent (Figure 1D,E).

https://doi.org/10.1021/acsomega.4c08884
ACS Omega 2025, 10, 7964−7972

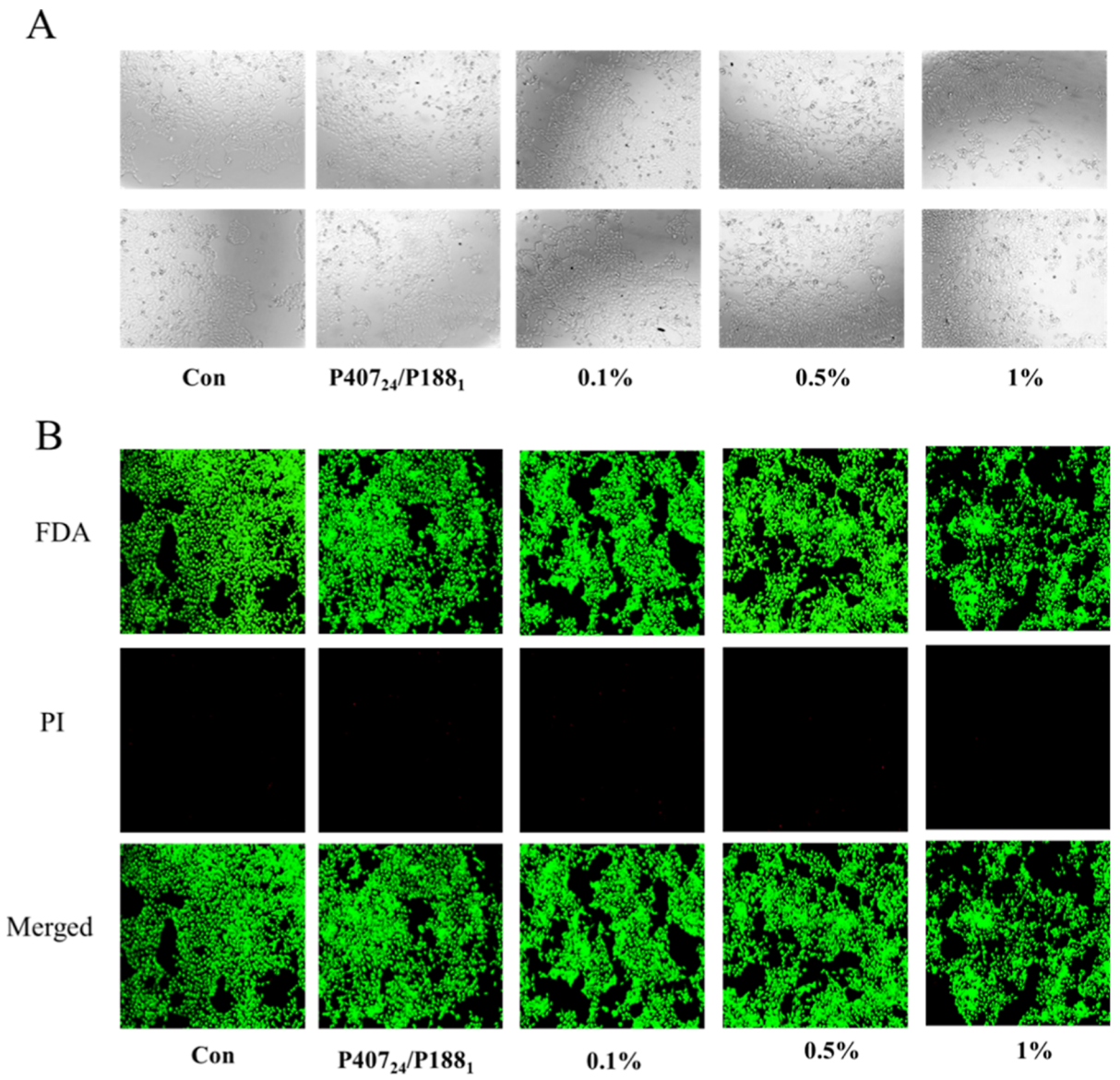

Figure 4. Biocompatibility and cytotoxicity of Car-P407$_{24}$/P188$_1$. (A) Cytocompatibility was observed by light microscopy, and (B) cytotoxicity was detected by a live/dead cell kit (live cells were stained green, dead cells were stained red).

3.2. Physicochemical Properties of Car-P407$_{24}$/P188$_1$. *3.2.1. Morphological Characteristics.* Sol−gel transition behavior was observed at room temperature and 32 °C by the tube-inversion method to evaluate the fluidity and viscosity of the hydrogel at different temperatures. Figure 2A shows the status of the Car-P407$_{24}$/P188$_1$ hydrogel after 2 min at 32 °C. It could be found that the hydrogel became a gel state under this condition, and there was still no liquid flow phenomenon after inverting the Eppendorf tube for 1 min, indicating the formation of a stable gel state. Rheometer measurements showed that the viscosity of Car-P407$_{24}$/P188$_1$ hydrogels gradually increased with the increase in the carvedilol content. However, it still maintained good fluidity at room temperature and stayed in the gel state after being placed at 32 °C for 60 ± 15 s (Figure 2A). Figure 2B,C shows the state of Car-P407$_{24}$/P188$_1$ after different days and ultrahigh speed centrifugation of the gel at room temperature, respectively. The drug-containing gel was centrifuged in an ultracentrifuge and refrigerated at 4 °C. The properties of the gel did not change significantly after 30 and 60 days, remaining homogeneous, clear, and transparent, and there was no delamination and precipitation, indicating that Car-P407$_{24}$/P188$_1$ possessed good stability.

3.2.2. SEM Observation of the Gel Microstructure. Generally, hydrogels possess a porous structure, which enables them to show good water absorption and retention properties and also enables them to possess good swelling properties. Figure 3A shows the SEM images of P407$_{24}$/P188$_1$ and Car-P407$_{24}$/P188$_1$. It could be found that the P407$_{24}$/P188$_1$ hydrogel freeze-dried substance was a regularly arranged tetragonal network structure of porous holes with a pore size range of approximately 8−12 μm. Notably, after the addition of carvedilol to the P40724/P1881 system, the internal network structure of Car-P40724/P1881 was not significantly altered (Figure 3A). The results indicate that carvedilol was physically bound and encapsulated in the porous structure of the poloxamer hydrogel.

3.2.3. FTIR Spectra of Car-P407$_{24}$/P188$_1$. Figure 3B shows the FTIR spectra of P407$_{24}$/P188$_1$, carvedilol, and Car-P407$_{24}$/P188$_1$. P407$_{24}$/P188$_1$ showed characteristic peaks at about 2882 cm^{-1} (C−H stretching) and 1102 cm^{-1} (C═O

https://doi.org/10.1021/acsomega.4c08884
ACS Omega 2025, 10, 7964−7972

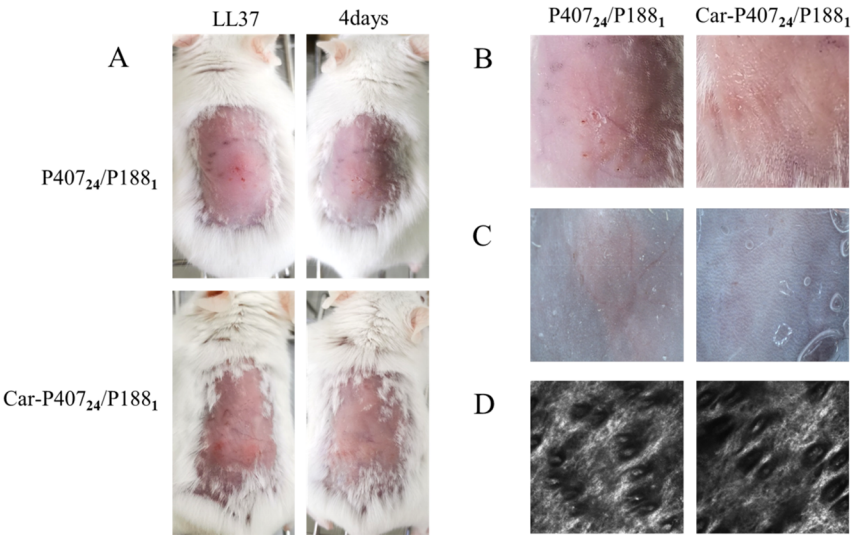

Figure 5. Carvedilol-containing thermosensitive hydrogel improves rosacea-like phenotype in mice. (A and B) Naked eye skin phenotypes, (C) dermoscopic phenotypes, and (D) reflective confocal microscopy phenotypes.

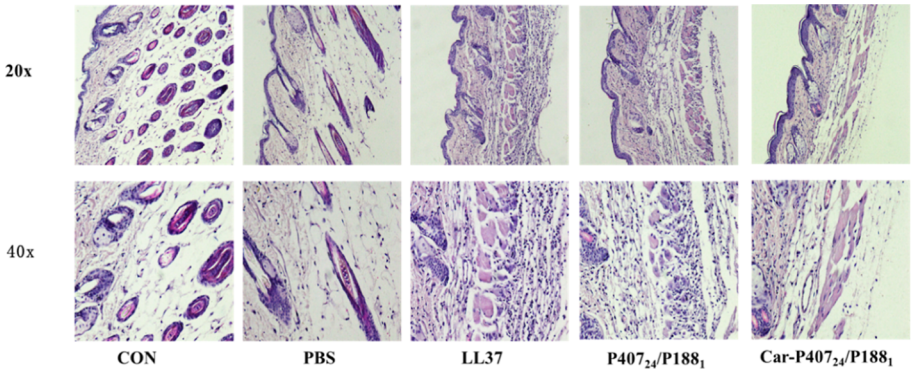

Figure 6. HE staining results of mouse skin tissues in each group.

stretching).[32,33] For pure carvedilol, the characteristic peaks at 3343 and 1587 cm^{-1} were attributed to N−H, O−H, and C=C, which was in agreement with the literature.[34] Notably, Car-P407$_{24}$/P188$_1$ showed characteristic peaks of carvedilol and P407$_{24}$/P188$_1$, suggesting that carvedilol was successfully introduced into the P407$_{24}$/P188$_1$ hydrogels.

3.2.4. Drug Release Capacity of Car-P407$_{24}$/P188$_1$. Figure 3C shows the cumulative drug release rate of Car-P407$_{24}$/P188$_1$. The cumulative release rates of Car-P407$_{24}$/P188$_1$ hydrogels with different drug content ratios were 86.54%, 75.66%, and 56.30%, respectively. Under neutral pH conditions, the results indicated a slow and sustained release of the drug with a high effective release rate (Figure 3C). However, as the percentage of drug content increased, the drug release rate started to decrease, which may be due to the saturation of the drug loading of the gel, where the actual drug loading rate was less than the theoretical loading rate.

3.2.5. Swelling Ratios of Car-P407$_{24}$/P188$_1$. Clinical studies had found that most patients with rosacea experience increased transdermal water loss, resulting in dry skin.[35,36] The hydrogel possessed good swelling properties and good water absorption and water retention properties, which could to a certain extent achieve the effect of skin moisturization. The water absorption of the material was conducted in its dried hydrogel state; the results of the swelling test show that Car-P407$_{24}$/P188$_1$ hydrogel exhibits a high SR, and it could reach 130−180% of the original mass (Figure 3D).

3.2.6. Cytotoxicity and Cytocompatibility of Car-P407$_{24}$/P188$_1$. Car-P407$_{24}$/P188$_1$ extracts with different drug-containing agglutinations were cocultured with HaCaT cells for 24 h. Figure 4A shows the cytocompatibility observed under a light microscope. It could be found that the cells grew well after the addition of different drug-containing ratios of Car-P407$_{24}$/P188$_1$ and fused in the gel for adherent growth, and the morphology of the cells did not change significantly (Figure 4A). Cells were furthermore evaluated for viability using Calcein AM and PI dyes, where green represented live cells and red represented dead cells (Figure 4B). Results showed that there was no massive cell death in any of the groups and there was no significant difference between the groups (Figure 4B). Taken together, these assays corroborated that Car-P407$_{24}$/P188$_1$ was nontoxic and possessed a favorable biocompatibility.

3.3. Efficacy of Car-P407$_{24}$/P188$_1$ in Rosacea Flushing and Erythema. To investigate whether the Car-P407$_{24}$/P188$_1$ hydrogel was efficacious against rosacea flushing and erythema, LL37 was injected subcutaneously into the dorsal skin of mice every 12 h four times to simulate a model of rosacea-like phenotype. The main pathological changes are inflammation and angiogenesis.[37] Significant erythema and telangiectasia were visible to the naked eye after LL37 injection. A purplish-

https://doi.org/10.1021/acsomega.4c08884
ACS Omega 2025, 10, 7964−7972

red background with a uniformly distributed vascular network was seen dermoscopically. Skin CT showed refractive streaks and scattered material in the hair follicles after LL37 injection, and neutrophils were seen around the follicles, surrounded by a nonspecific chronic inflammatory infiltrate. After 4 days of treatment with Car-$P407_{24}/P188_1$, both erythema and capillary dilation were significantly relieved in the treatment group (Figure 5A−C). The Car-$P407_{24}/P188_1$ hydrogel was demonstrated to significantly reduce the area of redness and score on the backs of rosacea-like mice. Rosacea is an inflammatory disease; inflammation and vascular disease are its main pathogenesis. Treatment with Car-$P407_{24}/P188_1$ resulted in a significant reduction in the inflammatory response described above, and both the refractive strip pattern within the hair follicle and the periphery with a nonspecific chronic inflammatory infiltrate were ameliorated (Figure 5D). Histological analysis revealed that the cellular infiltration in the skin of rosacea-like mice was significantly reduced after treatment with the Car-$P407_{24}/P188_1$ hydrogel (Figure 6), suggesting that the Car-$P407_{24}/P188_1$ hydrogel possesses a significant ameliorative effect on the rosacea-like phenotype in mice.

4. DISCUSSION

Rosacea is a common chronic inflammatory skin disease; it usually occurs after the age of 30. It is estimated to affect about 2−5% of adults worldwide.[38] Long-term facial flushing and erythema can cause serious physical discomfort and emotional distress, as well as heavy medical burden.[2] However, there is still no effective cure, and the treatment of persistent erythema and flushing remains a major challenge in clinical practice.[2,39] Several studies have shown a β-adrenergic receptor antagonist to be effective in reducing facial flushing and persistent erythema,[16] which may be an effective treatment for rosacea-associated facial flush and erythema. However, due to its wide range of systemic targets, side effects associated with the oral dosage form should not be overlooked, with bradycardia and hypotension being the most frequent adverse effects.[40] The Car-$P407_{24}/P188_1$ thermosensitive hydrogel studied in this experiment could control systemic adverse effects to a greater extent using topical administration, providing new ideas for erythematous, capillarised rosacea.

In recent years, the growing focus on individualized drug therapy and precision medicine has driven innovation in smart biomaterials.[41,42] The use of smart hydrogels in drug delivery systems reduces the frequency of administration, maintains the desired therapeutic concentration in a single dose, and minimizes drug side effects by preventing accumulation of the drug in nontarget tissues.[43,44] In addition, smart hydrogels are easy to prepare, making them ideal for sustained-release systems for doped drugs.[45] The Car-$P407_{24}/P188_1$ hydrogel takes advantage of these properties of hydrogels to achieve the effect of slow drug release.

In this work, the Car-$P407_{24}/P188_1$ thermosensitive hydrogel was prepared by the cold swelling method. By detecting the gel formation time and temperature, the ratio of P407 and P188 was adjusted to achieve the most suitable state for the topical gel for human skin. SEM results showed that the hydrogel possessed a porous structure, which provided a good reserve space for the drug. FTIR results showed that carvedilol exhibited N−H, O−H, and C═C absorption peaks at 3343 and 1587 cm^{-1}, and the characteristic peaks were also found in Car-$P407_{24}/P188_1$, which proved that carvedilol was successfully encapsulated by the hydrogel. In addition, Car-$P407_{24}/P188_1$ shows a good swelling property. The experiments show that it possesses the strongest water-absorbing ability in the first hour and reached a relative equilibrium state with the extension of time, which could play a role in skin moisturization. These characteristics can help moisturize the skin to a certain extent. Finally, toxicity testing confirmed that Car-$P407_{24}/P188_1$ was not significantly cytotoxic and had good cellular biocompatibility.

LL-37 plays an important role in innate immunity in rosacea inflammation.[1] LL-37 was injected subcutaneously into the dorsal skin of mice, and a model of the rosacea-like phenotype in mice was successfully constructed. Topical application of the Car-$P407_{24}/P188_1$ hydrogel was used to assess the skin status by dermoscopy and skin CT, which confirmed that Car-$P407_{24}/P188_1$ possesses better control of erythema and flushing. Subsequent HE staining of the tissues showed that Car-$P407_{24}/P188_1$ played an active role in the inflammation control process.

This work was only a preliminary validation of animal phenotype, but it has not been used in clinical patients. The optimal drug loading rate for therapeutic use must be confirmed by more studies. In conclusion, Car-$P407_{24}/P188_1$ exhibits a good therapeutic effect on rosacea-associated facial flushing and erythema. It possesses some anti-inflammatory properties and exhibits great potential for future use in rosacea treatment.

5. CONCLUSIONS

In conclusion, a temperature-sensitive hydrogel encapsulating carvedilol (Car-$P407_{24}/P188_1$) was obtained by the cold swelling method and was successfully used in the treatment of rosacea for topical application. The hydrogel possessed rich pore structures, which facilitated drug encapsulation to achieve slow release of the drug. In addition, the hydrogel exhibited good swelling, water absorption, and retention and possessed good biocompatibility and stability. Moreover, the temperature-sensitive property of Car-$P407_{24}/P188_1$ gave a good phase transition property, which enabled the realization of its rapid gel formation on the skin surface. In a skin rosacea therapeutic study with a mouse model, Car-$P407_{24}/P188_1$ significantly inhibited the nonspecific chronic inflammatory response, thereby demonstrating a favorable therapeutic effect on rosacea-associated facial flushing and erythema. The hydrogel showed great potential for the treatment of rosacea. This work provides new insights for the development of topical agents for the treatment of rosacea.

■ ASSOCIATED CONTENT

Data Availability Statement

All data generated or analyzed during this study are included in this published article (and its additional files).

■ AUTHOR INFORMATION

Corresponding Authors

Lechun Lyu − *Department of Yunnan Key Laboratory of Stem Cell and Regenerative Medicine, School of Rehabilitation, Kunming Medical University, Kunming 650500 Yunnan, China*; Phone: +086 0871 65922589; Email: lvlechun@kmmu.edu.cn

Dan Xu − *Department of Dermatology, First Affiliated Hospital of Kunming Medical University, Kunming 650032*

https://doi.org/10.1021/acsomega.4c08884
ACS Omega 2025, 10, 7964−7972

Yunnan, China; orcid.org/0009-0003-3953-339X; Phone: +086 0871 65329399; Email: drxudan@126.com

Authors

Huiya Chen − *Department of Dermatology, First Affiliated Hospital of Kunming Medical University, Kunming 650032 Yunnan, China*

Zhigang Zhang − *Department of Pharmacy, TCM-Integrated Hospital, Southern Medical University, Guangzhou 510315 Guangdong, China*

Jue Qi − *Department of Dermatology, First Affiliated Hospital of Kunming Medical University, Kunming 650032 Yunnan, China*

Can Cao − *Department of Dermatology, First Affiliated Hospital of Kunming Medical University, Kunming 650032 Yunnan, China*

Min Lin − *Faculty Metallurgy and Energy Engineering, Kunming University of Science and Technology, Kunming 650093 Yunnan, People's Republic of China*

Complete contact information is available at: https://pubs.acs.org/10.1021/acsomega.4c08884

Author Contributions

Huiya Chen: Conceptualization, Formal analysis, Investigation, Methodology, Visualization, Writing−original draft. Zhigang Zhang: Writing−review and editing. Jue Qi: Writing−review and editing. Can Cao: Writing−review and editing. Min Lin: Writing−review and editing. Dan Xu: Conceptualization, Resources, Supervision, Writing−review and editing. Lechun Lyu: Conceptualization, Resources, Supervision, Writing−review and editing.

Author Contributions

All procedures performed in studies involving animal experiments were in accordance with the ethical standards of the Ethics Committee of Kunming Medical University (approval date and number: 20.02.2019/KMMU2019315).

Author Contributions

All authors agree to publish this manuscript.

Funding

This work was supported by the National Natural Science Foundation of China [grant numbers 82160598, 81660518] and the Joint Key Program of Yunnan Provincial Department of Science and Technology−Kunming Medical University [grant number 202401AYO70001−035].

Notes

The authors declare no competing financial interest.

■ ACKNOWLEDGMENTS

The authors thank the Science and Technology Achievement Incubation Center, Kunming Medical University.

■ LIST OF ABBREVIATIONS

poloxamer 407, P407; poloxamer 188, P188; scanning electron microscopy, SEM; Fourier transform infrared spectrometry, FTIR; thermosensitive hydrogel encapsulated carvedilol, Car-$P407_{24}/P188_1$; polyoxyethylene, PEO; polyoxypropylene, PPO; phosphate buffered saline, PBS; percentage swelling rate, SR; human keratinocytes, HaCaT; antimicrobial peptide, LL37; standard deviation, SD; propidium iodide, PI

■ REFERENCES

(1) Yoon, S.-H.; Hwang, I.; Lee, E.; Cho, H.-J.; Ryu, J. H.; Kim, T.-G.; Yu, J.-W. Antimicrobial Peptide LL-37 Drives Rosacea-Like Skin Inflammation in an NLRP3-Dependent Manner. *J. Invest. Dermatol.* **2021**, *141* (12), 2885−2894.

(2) Wladis, E. J.; Adam, A. P. Immune Signaling in Rosacea. *Ocul. Surf.* **2021**, *22*, 224−229.

(3) Marchitto, M. C.; Chien, A. L. Mast Cell Stabilizers in the Treatment of Rosacea: A Review of Existing and Emerging Therapies. *Dermatol. Ther.* **2021**, *11* (5), 1541−1549.

(4) Sharma, A.; Kroumpouzos, G.; Kassir, M.; Galadari, H.; Goren, A.; Grabbe, S.; Goldust, M. Rosacea Management: A Comprehensive Review. *J. Cosmet. Dermatol.* **2022**, *21* (5), 1895−1904.

(5) Chinese Journal of Dermatology. Guidelines for the diagnosis and treatment of rosacea in China (2021 edition). *Chin. J. Dermatol.* **2021**, *54*, 279.

(6) Gether, L.; Overgaard, L. K.; Egeberg, A.; Thyssen, J. P. Incidence and Prevalence of Rosacea: A Systematic Review and Meta-Analysis. *Br. J. Dermatol.* **2018**, *179* (2), 282−289.

(7) Li, J.; Wang, B.; Deng, Y.; Shi, W.; Jian, D.; Liu, F.; Huang, Y.; Tang, Y.; Zhao, Z.; Huang, X.; Li, J.; Xie, H. Epidemiological Features of Rosacea in Changsha, China: A Population-Based, Cross-Sectional Study. *J. Dermatol.* **2020**, *47* (5), 497−502.

(8) Fei, W.; Han, Y.; Li, A.; Li, K.; Ning, X.; Li, C.; Wang, W.; Meng, R.; Cui, Y. Summarization and Comparison of Dermoscopic Features on Different Subtypes of Rosacea. *Chin. Med. J.* **2022**, *135* (12), 1444−1450.

(9) Yang, R.; Liu, C.; Liu, W.; Luo, J.; Cheng, S.; Mu, X. Botulinum Toxin A Alleviates Persistent Erythema and Flushing in Patients with Erythema Telangiectasia Rosacea. *Dermatol. Ther.* **2022**, *12* (10), 2285−2294.

(10) Chen, M.; Deng, Z.; Huang, Y.; Li, J. Prevalence and Risk Factors of Anxiety and Depression in Rosacea Patients: A Cross-Sectional Study in China. *Front. Psychiatr.* **2021**, *12*, 659171.

(11) Huang, Y.; Yan, S.; Xie, H.; Wang, B.; Zhao, Z.; Huang, Y.; Li, J. Health Related Quality of Life of Rosacea Patients in China Assessed by Dermatology Life Quality Index and Willingness to Pay. *Patient Prefer. Adherence* **2022**, *16*, 659−670.

(12) Zhou, L.; Zhao, H.; Zhao, H.; Meng, X.; Zhao, Z.; Xie, H.; Li, J.; Tang, Y.; Zhang, Y. GBP5 Exacerbates Rosacea-like Skin Inflammation by Skewing Macrophage Polarization towards M1 Phenotype through the NF-κB Signalling Pathway. *J. Eur. Acad. Dermatol. Venereol.* **2023**, *37* (4), 796−809.

(13) Liu, T.; Li, J.; Deng, Z.; Chen, M.; Sha, K.; Xiao, W.; Xie, H.; Zhao, Z. Increased Serum Levels of CCL3, CXCL8, CXCL9, and CXCL10 in Rosacea Patients and Their Correlation with Disease Severity. *J. Dermatol.* **2022**, *49* (5), 525−533.

(14) Logger, J. G. M.; Olydam, J. I.; Driessen, R. J. B. Use of Beta-Blockers for Rosacea-Associated Facial Erythema and Flushing: A Systematic Review and Update on Proposed Mode of Action. *J. Am. Acad. Dermatol.* **2020**, *83* (4), 1088−1097.

(15) Li, J.; Tang, J.-Y.; Fu, J.; Zhang, M.-W.; Wan, M.; Chen, D.-W.; Chen, Q.-Q.; Li, X.; Song, G.-J.; Ni, R.-R.; Song, Z.-Q. Carvedilol Ameliorates Persistent Erythema of Erythematotelangiectatic Rosacea by Regulating the Status of Anxiety/Depression. *J. Dermatol.* **2022**, *49* (11), 1139−1147.

(16) Seo, B. H.; Kim, D. H.; Suh, H. S.; Choi, Y. S. Facial Flushing and Erythema of Rosacea Improved by Carvedilol. *Dermatol. Ther.* **2020**, 33 (6), No. e14520.

(17) Llamas-Molina, J. M.; Ayén-Rodríguez, A. ·.; De la Torre-Gomar, F. J. RF - Carvedilol and Its Applications in Dermatology. *Actas Dermosifiliogr.* **2023**, *114* (10), 896−898.

(18) Casabella-Ramón, S.; Jiménez-Sábado, V.; Tarifa, C.; Casellas, S.; Lu, T. T.; Izquierdo-Castro, P.; Gich, I.; Jiménez, M.; Ginel, A.; Guerra, J. M.; Chen, S. R. W.; Benítez, R.; Hove-Madsen, L. Impact of R-Carvedilol on B2-Adrenergic Receptor-Mediated Spontaneous Calcium Release in Human Atrial Myocytes. *Biomedicines* **2022**, *10* (7), 1759.

(19) Hsu, C.-C.; Lee, J. Y.-Y. Carvedilol for the Treatment of Refractory Facial Flushing and Persistent Erythema of Rosacea. *Arch. Dermatol.* **2011**, *147* (11), 1258−1260.
(20) Zhang, J.; Jiang, P.; Sheng, L.; Liu, Y.; Liu, Y.; Li, M.; Tao, M.; Hu, L.; Wang, X.; Yang, Y.; Xu, Y.; Liu, W. A Novel Mechanism of Carvedilol Efficacy for Rosacea Treatment: Toll-Like Receptor 2 Inhibition in Macrophages. *Front. Immunol.* **2021**, *12*, 609615.
(21) Khoshnavay Foumani, M.; Amirshahrokhi, K.; Namjoo, Z.; Niapour, A. Carvedilol Attenuates Inflammatory Reactions of Lipopolysaccharide-Stimulated BV2 Cells and Modulates M1/M2 Polarization of Microglia via Regulating NLRP3, Notch, and PPAR-γ Signaling Pathways. *N. Schmied. Arch. Pharmacol.* **2024**, *397* (7), 4727−4736.
(22) Amarachinta, P. R.; Sharma, G.; Samed, N.; Chettupalli, A. K.; Alle, M.; Kim, J.-C. Central Composite Design for the Development of Carvedilol-Loaded Transdermal Ethosomal Hydrogel for Extended and Enhanced Anti-Hypertensive Effect. *J. Nanobiotechnol.* **2021**, *19* (1), 100.
(23) Agnihotri, S. A.; Aminabhavi, T. M. Development of Novel Interpenetrating Network Gellan Gum-Poly(Vinyl Alcohol) Hydrogel Microspheres for the Controlled Release of Carvedilol. *Drug Dev. Ind. Pharm.* **2005**, *31* (6), 491−503.
(24) Okwundu, N.; Cline, A.; Feldman, S. R. Difference in Vasoconstrictors: Oxymetazoline vs. Brimonidine. *J. Dermatol. Treat.* **2021**, *32* (2), 137−143.
(25) Lin, J.; Jiao, G.; Kermanshahi-Pour, A. Algal Polysaccharides-Based Hydrogels: Extraction, Synthesis, Characterization, and Applications. *Mar. Drugs* **2022**, *20* (5), 306.
(26) Brambilla, E.; Locarno, S.; Gallo, S.; Orsini, F.; Pini, C.; Farronato, M.; Thomaz, D. V.; Lenardi, C.; Piazzoni, M.; Tartaglia, G. Poloxamer-Based Hydrogel as Drug Delivery System: How Polymeric Excipients Influence the Chemical-Physical Properties. *Polymers* **2022**, *14* (17), 3624.
(27) Homayouni, A.; Amini, M.; Sohrabi, M.; Varshosaz, J.; Nokhodchi, A. Curcumin Nanoparticles Containing Poloxamer or Soluplus Tailored by High Pressure Homogenization Using Antisolvent Crystallization. *Int. J. Pharm.* **2019**, *562*, 124−134.
(28) Sunoqrot, S.; Orainee, B.; Alqudah, D. A.; Daoud, F.; Alshaer, W. Curcumin-Tannic Acid-Poloxamer Nanoassemblies Enhance Curcumin's Uptake and Bioactivity against Cancer Cells in Vitro. *Int. J. Pharm.* **2021**, *610*, 121255.
(29) Russo, E.; Villa, C. Poloxamer Hydrogels for Biomedical Applications. *Pharmaceutics* **2019**, *11* (12), No. E671.
(30) Cui, N.; Dai, C.-Y.; Mao, X.; Lv, X.; Gu, Y.; Lee, E.-S.; Jiang, H.-B.; Sun, Y. Poloxamer-Based Scaffolds for Tissue Engineering Applications: A Review. *Gels* **2022**, *8* (6), 360.
(31) Vanderstraeten, M. C. M.; Gutermuth, J.; Grosber, M. Contact Anaphylaxis to Poloxamer 188 and 407 in a Periodontal Gel. *Contact Dermat.* **2021**, *85*, 253.
(32) Luo, Y.; Teng, Z.; Li, Y.; Wang, Q. Solid Lipid Nanoparticles for Oral Drug Delivery: Chitosan Coating Improves Stability, Controlled Delivery, Mucoadhesion and Cellular Uptake. *Carbohydr. Polym.* **2015**, *122*, 221−229.
(33) Bujňáková, Z.; Dutková, E.; Baláž, M.; Turianicová, E.; Baláž, P. Stability Studies of As4S4 Nanosuspension Prepared by Wet Milling in Poloxamer 407. *Int. J. Pharm.* **2015**, *478* (1), 187−192.
(34) Pešić, N.; Dapčević, A.; Ivković, B.; Kachrimanis, K.; Mitrić, M.; Ibrić, S.; Medarević, D. Potential Application of Low Molecular Weight Excipients for Amorphization and Dissolution Enhancement of Carvedilol. *Int. J. Pharm.* **2021**, *608*, 121033.
(35) Wang, J.; Sun, Y.; Chen, L.; Wang, Y.; Shi, D.; Wu, Y.; Gao, X. Supramolecular Salicylic Acid Ameliorates Rosacea-like Eruptions by Suppressing NLRP3-Mediated Inflammasome Activation in Mice. *Int. Immunopharmacol.* **2023**, *118*, 110057.
(36) Hu, M.; Tu, Y.; Man, M.-Q.; He, Y.; Wu, P.; He, L.; Gu, H. Rosacea and Seborrheic Dermatitis Differentially Respond to Lactic Acid Sting and Capsaicin Tests in Chinese Women. *J. Cosmet. Dermatol.* **2023**, *22* (12), 3505−3510.
(37) Wang, L.; Wang, Y.-J.; Hao, D.; Wang, X.-Y.; Li, X.-X.; Zhao, Q.; Li, Y.-M.; He, G.; Jiang, X. Long Non-Coding RNA NEAT1 Functions as a Competing Endogenous RNA to Regulate S100A9 Expression by Sponging miR-196a-5p in Rosacea. *J. Dermatol. Sci.* **2021**, *102* (1), 58−67.
(38) Marchitto, M. C.; Chien, A. L. Mast Cell Stabilizers in the Treatment of Rosacea: A Review of Existing and Emerging Therapies. *Dermatol. Ther.* **2021**, *11* (5), 1541−1549.
(39) Pietschke, K.; Schaller, M. Long-Term Management of Distinct Facial Flushing and Persistent Erythema of Rosacea by Treatment with Carvedilol. *J. Dermatol. Treat.* **2018**, *29* (3), 310−313.
(40) Bunchorntavakul, C.; Reddy, K. R. Pharmacologic Management of Portal Hypertension. *Clin. Liver Dis.* **2019**, *23* (4), 713−736.
(41) Montoya, C.; Du, Y.; Gianforcaro, A. L.; Orrego, S.; Yang, M.; Lelkes, P. I. On the Road to Smart Biomaterials for Bone Research: Definitions, Concepts, Advances, and Outlook. *Bone Res.* **2021**, *9* (1), 12.
(42) Bordbar-Khiabani, A.; Gasik, M. Smart Hydrogels for Advanced Drug Delivery Systems. *Int. J. Mol. Sci.* **2022**, *23* (7), 3665.
(43) Krishnan, N.; Fang, R. H.; Zhang, L. Engineering of Stimuli-Responsive Self-Assembled Biomimetic Nanoparticles. *Adv. Drug Delivery Rev.* **2021**, *179*, 114006.
(44) Zarrintaj, P.; Ramsey, J. D.; Samadi, A.; Atoufi, Z.; Yazdi, M. K.; Ganjali, M. R.; Amirabad, L. M.; Zangene, E.; Farokhi, M.; Formela, K.; Saeb, M. R.; Mozafari, M.; Thomas, S. Poloxamer: A Versatile Tri-Block Copolymer for Biomedical Applications. *Acta Biomater.* **2020**, *110*, 37−67.
(45) Jacob, S.; Nair, A. B.; Shah, J.; Sreeharsha, N.; Gupta, S.; Shinu, P. Emerging Role of Hydrogels in Drug Delivery Systems, Tissue Engineering and Wound Management. *Pharmaceutics* **2021**, *13* (3), 357.

https://doi.org/10.1021/acsomega.4c08884
ACS Omega 2025, 10, 7964−7972